RSC Sustainability

ROYAL SOCIETY OF CHEMISTRY

PAPER

View Article Online
View Journal | View Issue

Cite this: *RSC Sustainability*, 2025, **3**, 4561

Transforming aluminium waste: sustainable conversion to commercial MOFs, hydrogen fuel, and essential aluminium feedstocks

M. C. Lawrence, R. S. Horne and B. A. Blight *

Received 29th July 2025
Accepted 7th August 2025

DOI: 10.1039/d5su00631g

rsc.li/rscsus

Aluminium dross waste is generated during the aluminium smelting process and has an annual production of nearly 5.3 M tonnes worldwide. It is largely comprised of aluminium but also contains different metal oxides, silicates, and other impurities. We demonstrate how to make use of dross by producing high-value products (hydrogen gas, aluminium formate, aluminium acetate, aluminium hydroxide, MOF-303, Al-Fum) towards decarbonization of the aluminium industry. We produce hydrogen gas (1.1–1.2 L g^{-1} of dross) by digesting it with NaOH, while further outlining methods to upcycle this encased aluminium into high value materials, and identify a route to pure amporhous Al_2O_3 *via* aluminium formate or aluminium acetate. We also demonstrate the production of the water harvesing MOF-303 and Al-Fum directly from processed dross as the aluminium source. This study highlights a complete overview of upcycling of aluminium dross to high value products towards a green energy shift, and industrial circircular economy.

Sustainability spotlight

The aluminum smelting industry generates a large amount of dross (approximately 5.3 M tonnes per year), a side product that is rich in aluminum, iron, magnesium and other metal ions. Although some recycling efforts exist, they require expensive equipment or are very energy intensive resulting in much of the dross being discarded as waste. This work illustrates a closed loop, low energy process to up-cycle dross into high-value aluminum compounds, specifically aluminum based porous materials. This work also highlights a route for calcination of aluminum-based materials to alumina at much lower temperatures than currently used in industrial procedures (SDG 12). In addition, white hydrogen fuel, an attractive carbon free energy source is generated (SDG 7).

Aluminium is one of the most abundant elements present in the earth's crust, and is heavily used in the automotive, consumer, construction, and electronics industries.[1] Source aluminium exists mainly as aluminium oxide or aluminosilicates in minerals such as bauxite, containing a combination of gibbsite, boehmite and diaspora ($Al(OH)_3$, γ-AlO(OH), α-AlO(OH)).[2,3] Aluminium in its crude mineral state does not have properties desirable for industrial applications and must be processed to obtain pure aluminium.

The two main processes of aluminium production are the Bayer process, in which bauxite is converted to aluminium oxide (alumina; Al_2O_3) by calcination of aluminium hydroxide (from Bauxite) at temperatures above 1000 °C,[4] and the Hall–Héroult process where aluminium oxide is reduced to aluminium(0) (electrolysis at 900 °C; 13 Mwh kg^{-1}).[5] During the Hall–Héroult process a side product, termed dross, is produced. Dross is a combination of pure aluminium and other aluminium species (oxide, carbide, nitride), along with other metal oxides and silicates.[6] Depending on the aluminium content, it is labelled as white or black dross. White dross typically contains between 50 and 80% recoverable aluminium while black dross contains much less (7–50%).[7] During aluminium smelting it is estimated that dross is produced in 6–8% of total amount of aluminium produced.[8] Canada, a major producer of aluminium, produced an estimated 250 000 tonnes of dross in 2022, while the global dross production estimated at 5.3 M tonnes.[9] Much of this dross is untreated and put in landfill, posing environmental risks.[10,11] Given that dross is largely comprised of valuable materials, it should not be treated as landfill. Recycling efforts for dross do exist, focusing on recovering pure aluminium or alumina. These methods tend to be energy intensive and have not been well implemented due to high cost of infrastructure and operation.[12] The most popular dross upcycling method involves a rotary salt furnace, allowing separation of aluminium from the other elements in the dross.[13] Dross has been used as an additive to building materials including, cement, bricks and ceramics. Adding dross to these materials increases their corrosion resistance, fire retardation, and strength.[14]

We describe here that through the digestion of dross we form hydrogen gas – carbon-free energy dense gas, and an extremely attractive fuel source – and aluminium hydroxide – a common reagents used in pharmaceuticals, cosmetics, fire

Department of Chemistry, University of New Brunswick, Fredericton, New Brunswick, E3B 5A3, Canada. E-mail: b.blight@unb.ca

retardants and feedstock materials in the chemical industry.[15–17] We demonstrate direct conversion of this aluminium hydroxide to aluminium-based metal–organic frameworks (MOFs), which are a class of porous solids (akin to zeolitic materials) that have a robust variety of applications ranging from drug delivery, catalyst, and gas storage.[18,19] We also report that bulk low-temperature calcination of these framework materials produces high-purity aluminium oxide, another commercial commodity material. In short, we synergistically produce several high-value materials from dross, in a low-energy, low-waste route towards a decarbonized zero-waste aluminium smelting industry (Fig. 1).

Results and discussion

Dross characterization

Dross samples isolated from different locations on the production line were obtained from Rio Tinto Alcan (Quebec, Canada). Since variables throughout the Bayer and Hall–Héroult processes can alter compositional concentrations in the sample, it is important to determine the aluminium content of the dross samples. This was determined through micro-X-ray fluorescence (uXRF). Point source measurements indicated parts of the sample contained up to 98% aluminium, but isolated dross is not expected to be a completely homogeneous material, therefore uXRF surface maps of the samples were obtained to determine a more representative elemental composition of the dross,[8,20,21] indicating approximately 75 weight % aluminium on sample surface (see SI Tables S1–S4 for full uXRF breakdown).

To further understand the makeup of the dross samples, powder X-ray diffraction (PXRD) patterns of finely ground dross were collected (Fig. 2). The crystalline phases of dross was identified as aluminium oxide, pure aluminium, magnesium aluminium oxide, iron oxide, and magnesium oxide. The compounds identified in the diffractograms agree with the elements detected through uXRF.

While samples contain high amounts of Al, Mg, Na, and, Fe, they also contain a considerable amount of oxygen. Aluminium is an oxyphilic compound, and during dross formation it is oxidized to from an outer layer of aluminium oxide.[22] This outer layer prevents the reaction between water and aluminium and must be removed for efficient generation of hydrogen gas. Reports in the literature suggest using mechanochemical milling to remove the outer oxide layer, exposing the aluminium encased in the dross.[23,24] Other procedures suggest using a caustic solution (potassium/sodium hydroxide) to remove the outer oxide layer exposing the pure aluminium.[11,25] We used a combination of both these methods to provide a quick, and near quantitative generation of hydrogen gas.

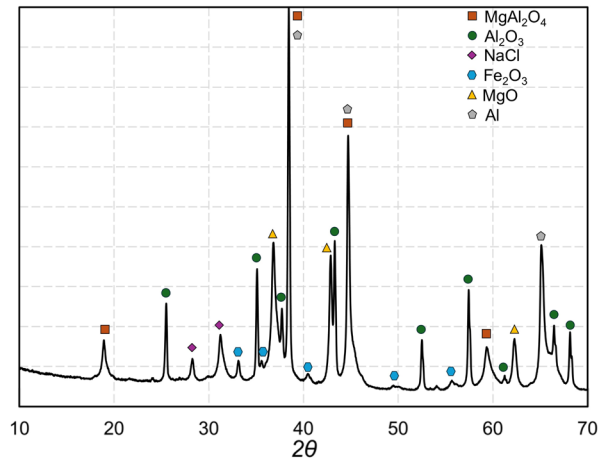

Fig. 2 Powder X-ray diffraction of dross after milling.

Hydrogen generation

As noted, the first high value product obtained in our process is hydrogen gas. Pure aluminium reacts slowly with water (eqn (1)) to produce hydrogen gas and aluminium hydroxide; a major component of the waste dross is aluminium making it the ideal material for sustainable hydrogen generation.[11,26] Previous work examining the hydrogen generation from black dross displayed as much as 0.6 litres of hydrogen per gram of dross.[11,23,24] By reacting the aluminium dross in a solution of sodium hydroxide, the process is accelerated where hydrogen gas and

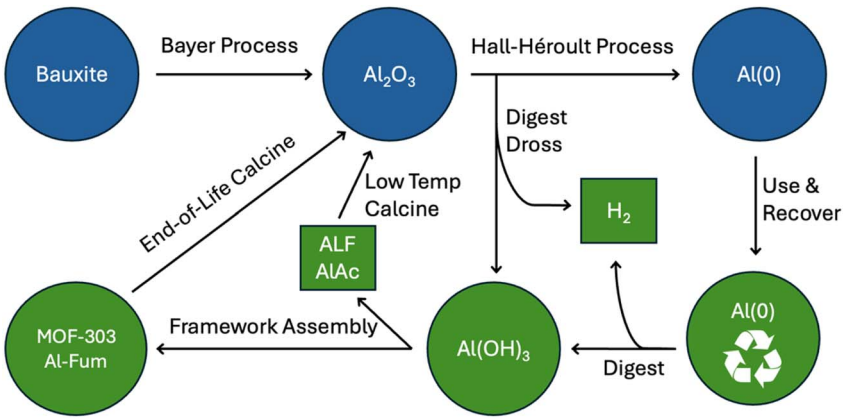

Fig. 1 Flow diagram of described closed-loop approach towards a zero-waste aluminium industry.

other value-add materials are produced (eqn (2)), such as sodium aluminium hydroxide.[11,21,27,28] which is in equilibrium with aluminium hydroxide and sodium hydroxide (eqn (3)).

$$Al_{(s)} + 3H_2O_{(l)} \rightarrow \frac{3}{2}H_{2(g)} + Al(OH)_{3(aq)} \quad (1)$$

$$Al_{(s)} + 3H_2O_{(l)} + NaOH_{(aq)} \rightarrow \frac{3}{2}H_{2(g)} + Na\left[Al(OH)_4\right]_{(aq)} \quad (2)$$

$$Na[Al(OH)_4]_{(aq)} \leftrightarrow Al(OH)_3(aq) + NaOH(aq) \quad (3)$$

To evaluate the amount of hydrogen produced by digesting white dross, water displacement measurements were performed at room temperature and atmospheric pressure (details in SI, Fig. S1).[11,20] The reaction was allowed to proceed overnight, ensuring complete digestion of the dross. The results are summarized in Table 1. Samples 1, 2, and 4 demonstrated similar hydrogen generation values. On average these samples generated 1.1–1.2 litres of hydrogen per gram of dross. This is equivalent to 12–13 MJ of energy from one kilogram of dross.

The purity of the hydrogen gas was also evaluated though gas chromatography. The gas was comprised mainly of hydrogen (92.6%), oxygen (1.5%) and nitrogen (5.9%). We attribute the presence of oxygen and nitrogen to ambient air in the sample. In atmospheric air, a typical ratio of approximately 4 : 1 nitrogen to oxygen is present, which was observed (in much lower concentrations) in the gas samples collected. The hydrogen purity was comparable to previously reported values of hydrogen generated from black dross (93.2 mol%).[21]

Production of aluminium hydroxide

A second high-value product from this reaction is aluminium hydroxide. As noted above, the current industrial route to produce aluminium hydroxide from bauxite is through the Bayer process, which is high in energy and requires the use of additional reagents.[4]

Aluminium hydroxide is soluble in both acidic and basic media, but precipitates in neutral pH. Industrially, neutralizing a high pH system requires large amounts of acid and poses significant safety risks. We make use of the dissolution properties of aluminium hydroxide and its equilibrium with sodium aluminium hydroxide as outlined in eqn (2) and (3), respectively, and induce precipitation as saturation occurs, further driving disproportion of $NaAl(OH)_4$ to make $Al(OH)_3$. Previous reports outline this strategy, but have inaccurately identified the resulting precipitate as aluminium oxide, or as a broader aluminium oxygen species.[28,29] David and Kopac demonstrated that the digestion of black dross leads to the formation of aluminium oxide hydroxide, which is different from the aluminium hydroxide isolated in this work.[11]

We characterized our aluminium hydroxide precipitate with uXRF, revealing aluminium and oxygen (38.5% and 60.1% respectively SI Table S9) as the major components, along with trace amounts of magnesium, sodium, and iron. These results agree with the obtained PXRD pattern (Fig. 3), displaying major signals for aluminium hydroxide, along with peaks representing magnesium oxide, magnesium aluminium oxide, and aluminium oxide. These patterns are a qualitative representation of the sample and display the crystalline materials present.[30]

Recycling sodium hydroxide

As noted, eqn (3) illustrates the equilibrium that exist between sodium aluminium hydroxide and sodium hydroxide. This equilibrium heavily favours the products side, generating more aluminium hydroxide and liberating sodium hydroxide, functioning as a catalyst in propagating the reaction. As such, during the reaction the filtrate containing NaOH is continuously recycled, creating a near zero waste aspect. The collected NaOH solution has been re-used five times in our experiments with minimal change in pH and negligible differences in volume of hydrogen gas produced. By recycling the sodium hydroxide solution, we sustainably of produce high-value products while minimizing the amount of waste generated and energy used. This provides a low-energy and low-waste route to high-value products.

Upcycling aluminium: framework materials and alumina

The final stage of the Bayer process involves the calcination of aluminium hydroxide to produce Al_2O_3. This calcination is

Table 1 Hydrogen production from dross digestion and weight percent aluminium present in the analysed dross

Dross sample	H_2 produced from dross (L g^{-1})	wt% Al in dross[a]
1	1.2	75.69
2	1.1	78.58
3	0.87	75.80
4	1.2	80.18

[a] Based on uXRF mapping measurements.

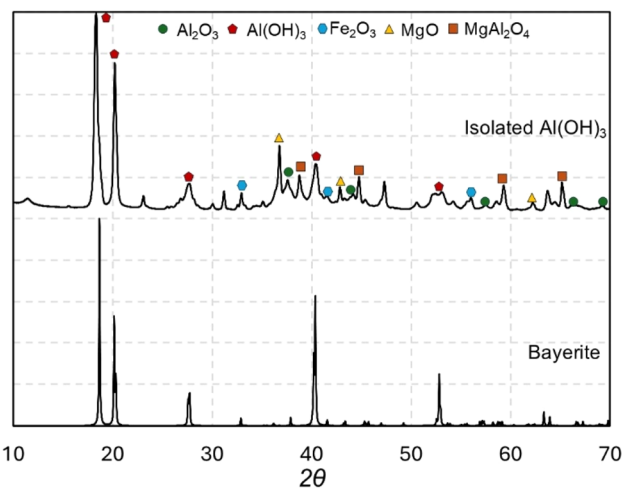

Fig. 3 Powder X-ray diffraction pattern of isolated aluminium hydroxide (top) and simulated powder X-ray diffraction pattern of Bayerite ($Al(OH)_3$, bottom).

done at temperatures in excess of 1000 °C, requiring tremendous amounts of energy input. Our work uses the isolated aluminium hydroxide as a building block for new aluminium-based framework materials. In this process we identified aluminium formate (ALF) and aluminium acetate (AlAc) each with their own industrial relevance. These compounds have a decomposition (calcination) temperature much lower than aluminium hydroxide, producing Al_2O_3 at half of the temperatures required for the conventional Bayer process. Furthermore, the synthesis of these materials provides a unique pathway to remove both soluble and insoluble impurities in generating high purity Al_2O_3.

ALF and AlAc

We synthesized ALF directly from our digested dross using a modified literature procedure.[31] Crude aluminium hydroxide isolated from dross was refluxed in formic acid overnight resulting in a white precipitate. This precipitate was characterized by uXRF (Table S5), PXRD (Fig. 4A), and TGA (Fig. S2) to confirm the successful synthesis. The decomposition of ALF under heating in air *via* TGA and occurred above 350 °C (Fig. S2), with a mass loss of 71.5% was observed (theoretical value of 69%). To characterize the resulting material, a sample of ALF was heated at 600 °C overnight to ensure the complete conversion of a larger mass of sample. The white powder that remained was then characterized though uXRF and PXRD. uXRF indicated remaining material is primarily comprised of aluminium and oxygen in ratios that correspond to Al_2O_3. The PXRD pattern of heated ALF was significantly different than that of as-synthesised ALF and crystalline Al_2O_3. Qualitatively, major peaks observed in the PXRD pattern correspond impurities identified in the original dross mixture (aluminium oxide, aluminium, magnesium aluminium oxide, and magnesium oxide), with a large drift in the baseline signal which is consistent with the presence of an amorphous material.[32] After uXRF and PXRD analysis, we conclude that we have indeed produced amorphous Al_2O_3, with the sample comprised primarily of aluminium, oxygen, and small amounts of magnesium (39.5, 52.5 and 6.3 wt%, respectively).

Aluminium hydroxyacetate (AlAc) was also synthesized similarly to previous literature procedures.[32] Our crude aluminium hydroxide was refluxed in concentrated glacial acetic acid overnight. The resulting precipitate was then isolated by suction filtration and characterized by uXRF (Table S10), PXRD (Fig. 4B), and TGA (Fig. S3). The obtained PXRD pattern matches the literature for aluminium hydroxyacetate ($Al(OH)(CH_3COO)_2$). uXRF of the crude AlAc indicates the sample is mainly comprised of aluminium, with small amounts of titanium, and iron metals (85.45, 9.07 and 3.22 weight percent respectively. See Table S10 for full sample composition). This remains consistent with the observations of ALF synthesized directly from the $Al(OH)_3$ precipitated from dross digestion. The TGA of the resulting compound showed a mass loss of 68.8%, within close agreement of the theoretical value of 68.3% and close to the reported value of 68.2%, confirming the formation of $Al(OH)(CH_3COO)_2$.[32] The synthesized AlAc was then heated above its decomposition temperature (600 °C) and the resulting powder was characterized through PXRD and uXRF, with powder pattern no longer matches that of AlAc, and only signals of impurities remain. uXRF of the calcined material indicated the metal contaminants to primarily be titanium and iron (see Table S11 for full composition).

Purification of $Al(OH)_3$ and implications

Converting aluminium species ($Al(OH_3)$, $AlO(OH)$ into Al_2O_3 through the calcination process has been well established in the literature.[32] Direct calcination of the dross derived aluminium hydroxide would result in Al_2O_3 containing a large amount of impurities while synthesizing ALF and AlAc with impurities is also undesirable, further leading to an impure Al_2O_3 after heating. This would rule out their direct reintroduction into the Hall–Héroult process if so desired. We were able to overcome this problem and remove the insoluble impurities by dissolution of aluminium hydroxide and filtration. The ALF and AlAc

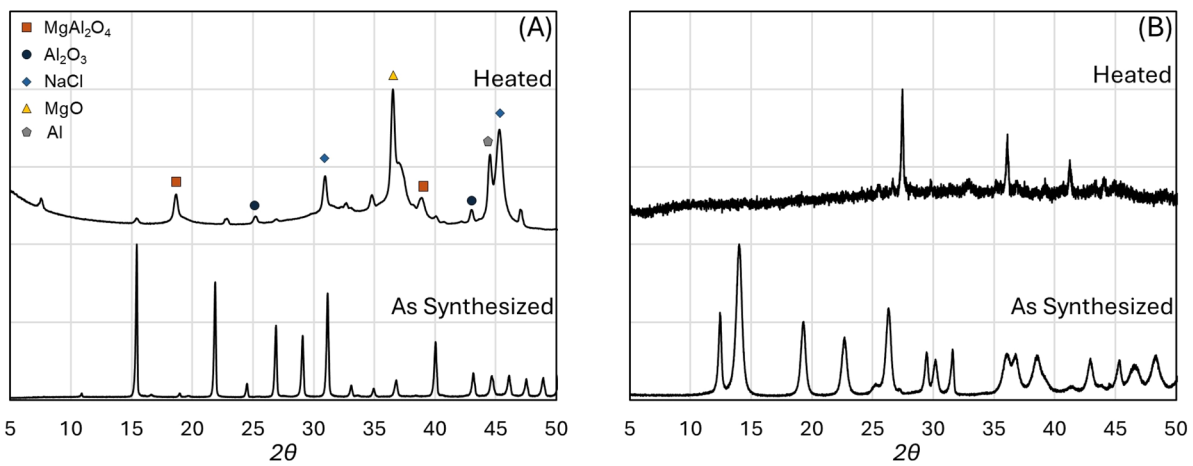

Fig. 4 Powder X-ray diffraction patter of ALF (A) as synthesized (bottom) and after heating at 600 °C overnight (top) and AlAc (B) as synthesized (bottom) and after heating at 600 °C overnight (top).

protocol also remove soluble impurities as the aluminium substrate is the only reactive metal species. As such, ALF was synthesized at a loading of 10 : 1 : 1 ($Al(OH)_3$: CHOOH : H_2O w : v : w), followed by heating for 3 minutes at 110 °C. Once the heating phase was complete, the insoluble impurities were separated from the filtrate. The filtrate, now containing dissolved aluminium hydroxide and formic acid, was returned to heating at 110 °C. Once the heating was complete, the white precipitate was isolated and identified as ALF *via* PXRD (Fig. 5A). The approach to synthesising pure AlAc, however, differed slightly from ALF. During the heating of $Al(OH)_3$ in glacial acetic acid the AlAc would precipitate faster than $Al(OH)_3$ dissolution, inhibiting filtration of insoluble impurities. To overcome this, the impure $Al(OH)_3$ was heated in concentrated hydrochloric acid over the course of 2 hours. At this point the $Al(OH)_3$ was dissolved, leaving solid impurities to be removed by suction filtration. A white precipitate was isolated after neutralisation with sodium hydroxide. This precipitate was added to excess glacial acetic acid and heated overnight resulting in a white precipitate, identified as AlAc (Fig. 5D).

The observed PXRD diffractograms for both ALF and AlAc showed their respective dominant phase regardless of the purification step being performed or not. This is due to the ALF or AlAc being the main component to the sample, dwarfing trace impurity signals. To ensure that all impurities were removed the samples were heated at 400 °C (Fig. 5B and E) and 600 °C (Fig. 5C and F) overnight. At these temperatures the ALF or AlAc would convert to the non-crystalline Al_2O_3, while crystalline impurities would be detected. Calcination of the purified ALF and AlAc resulted in PXRD patterns with no trace of previously observed impurities (Fig. 5). The patterns show no discernible crystalline phases, but instead baseline drift, indicating the presence of the dominant amorphous Al_2O_3 phase,[30,32] and confirmed by uXRF. uXRF of ALF heated at 400 °C or 600 °C showed approximately 35 and 47 weight % for aluminium and oxygen respectively (see Table S7 and S8 for full breakdown). Heated AlAc revealed a metal content of 99.45 weight % aluminium, which would correspond to 99.59% Al_2O_3 (see S12 and S13). The uXRF results demonstrate how effective this approach to the purification of $Al(OH)_3$ is, and its impact on the production of pristine ALF, AlAc, and high-purity Al_2O_3, above 99.5% pure a requirement for the Hall–Héroult process.

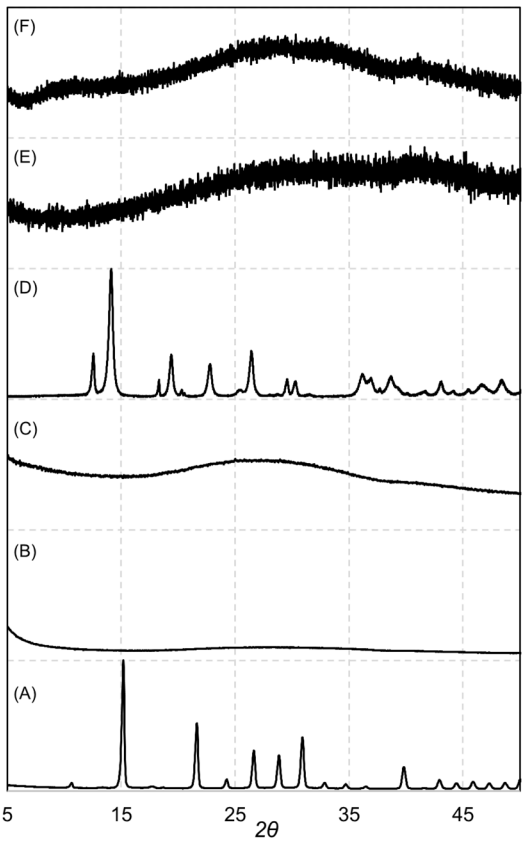

Fig. 5 Powder X-ray diffraction patterns of ALF and AlAc synthesized *via* purification methods (A and D) followed by heating at 400 °C or 600 °C overnight (ALF B and C, AlAc E and F, respectively).

MOFs directly from dross

The isolated aluminium hydroxide is an ideal building block to many other aluminium containing MOFs, including ALF (as described above), MOF-303, and Al-Fum. MOF-303 is an aluminium 1-*H*-pyrazole-3,5-dicarboxylate porous material that has gained much attention for its water harvesting capabilities. It was first reported in 2018 by Yaghi and coworkers,[33] and has been shown to produce up to 1.3 L of water per Kg of MOF per day from the atmosphere at 32% relative humidity.[34,35] MOF-303 shows great potential in providing a source of fresh water to arid, and water depleted regions over the world. We envision making this product from a waste stream, showing how we can further elevate the sustainable impact of this innovation.

Yaghi's traditional synthesis reacts aluminium chloride and sodium hydroxide, generating aluminium hydroxide *in situ*.[36] The route outlined in this work generates aluminium hydroxide from the reaction of aluminium waste with sodium hydroxide, removing the reliance on aluminium chloride and adding a layer of sustainability to the synthesis. To ensure pure MOF production, we perform the dross digestion at a ratio of 1 g of dross per 10 mL of 1 M sodium hydroxide solution. At this concentration the aluminium hydroxide remains soluble, and the insoluble impurities are easily removed. The concentration of sodium hydroxide used to digest the aluminium waste in is much higher than the concentration used in the typical synthesis of MOF-303, thus diluting the aluminium hydroxide solution with water at a ratio of approximately 1 : 11.5 achieves the aluminium and sodium hydroxide concentrations established in previous protocols.[36] The ligand was then added following established literature ratios, followed by heating overnight yielded a white powder. Once washed with water and alcohol (methanol or ethanol) pure MOF-303 was obtained (Fig. S4 and S5).[36]

Al-Fum combines an aluminium centre with a fumaric acid as a ligand, and is an industrially relevant MOF produced at scale by BASF (BASF A 520).[37] Al-Fum has shown potential for CO_2 adsorption from wet gas streams, photocatalytic hydrogen production, and chlorofluorocarbons adsorption and

Table 2 Current method improvements highlighted in this work

	Current methods	This work
MOF-303 synthesis	$AlCl_3$ (ref. 36)	White dross
Al-Fum synthesis	$Al(SO_4)_3{\cdot}9H_2O$[39]	White dross
ALF and AlAc synthesis	$Al(OH)_3$ (ref. 31 and 32)	White dross
Calcination temperatures	Ca. 1000 °C[40]	Ca. 600 °C
Hydrogen production	N/A	1.2 L g^{-1} dross
$Al(OH)_3$ isolation	Heat, water, seed crystals[4]	Spontaneous precipitation
$Al(OH)_3$ purification	N/A	ALF, AlAc synthesis
Dross uses	Some recovery efforts, landfill[11]	White H_2 gas, $Al(OH)_3$ isolation, porous materials, Al_2O_3

selectivity.[37–39] The synthesis that BASF preforms on the tonne scale uses aluminium sulphate and sodium hydroxide to generate aluminium hydroxide *in situ.*[37] Using the same procedure as highlighted for MOF-303, we produced a solution of aluminium hydroxide, that was diluted with water at a ratio of 1 : 20 to synthesize Al-Fum from waste aluminium, adding a layer of sustainability to this industrial synthesis.

The synthesis of both MOFs was confirmed *via* N_2 adsorption measurements. Both MOF-303 and Al-Fum produced a type I isotherm, and a calculated BET surface area of 1450 and 850 m^2 g^{-1} respectively (Fig. S4).[36,39] Both calculated values agree with previously published literature values of 1300 and 965 m^2 g^{-1} respectively.[36,39] PXRD pattern of our synthesized material match those published in the literature (Fig. S5).[36,39] It should be noted that both these MOF can be calcined above 600 °C to produce γ-Al_2O_3 once the MOFs have reached end of life.[36,39]

Direct comparison

This work improves on current literature methods for the synthesis of MOF-303 and Al-Fum by using waste aluminium instead of $AlCl_3$ and $Al(SO_4){\cdot}9H_2O$ as the respective aluminium source, reducing the waste generated in the process, and eliminating the need for commodity chemicals.[36,39] Furthermore, we have presented a method to reduce the amount of dross introduced into the landfill by processing it at ambient temperatures and pressures to produce 1.2 litres of white hydrogen fuel per gram of dross, an untapped source of a carbon free fuel. This work also demonstrates the lowering of calcination temperatures to from Al_2O_3 from over 1000 °C to 600 °C by converting the isolated $Al(OH)_3$ to ALF or AlAc.[40] This process also removes any impurities to ensure the synthesis of pure Al_2O_3 (Table 2).

Conclusions

In this work, we demonstrated a true closed loop approach to producing high-value products from aluminium waste material, contributing directly to the UN Sustainability Development Goals 7 and 12.[41] We began by producing near quantitative high purity hydrogen gas formation from white aluminium dross and a sodium hydroxide solution, a known process. We ascertained that the sodium hydroxide solution is not consumed in the reaction, and it can be reused near indefinitely (catalytic). We show that the aluminium hydroxide can be used to form ALF and AlAc, two upcycled materials with industrial relevance. We also make use of ALF and AlAc as feedstock materials for conversion to aluminium oxide at a much lower temperature (400 °C) than the industrially used Bayer process (1000 °C). This offers significant energy savings. We demonstrate the assembly of the highly publicised MOF-303 and Al-Fum through solvothermal routes directly from waste dross as the aluminium source, further adding to the high value products generated from this process.

Our findings show that there remains a significant fuel source (64 PJ of energy in the form of hydrogen) and other value-add materials to be drawn globally from the 5.3 M tonnes of aluminium dross waste being produced annually. This does not account for secondary domestic or commercial aluminium waste materials (including drinking vessels and other aluminium salvage) that require recycling, an area we are now looking to capture in the design of bench and pilot scale processes.

Author contributions

MCL: conceptualization, experimental, data collection and analysis, manuscript writing and preparation; RSH: experimental, data collection and analysis, writing; BAB: funding procurement, conceptualization, writing.

Conflicts of interest

Intellectual property protection has been filed in the form of a PCT application by UNB, BAB, and MCL, covering all novel aspects of the presented work.

Data availability

The raw data that underpins this work can be accessed through the University of New Brunswick data repository found here: **https://doi.org/10.25545/ZCXQMO**.

Supplementary information containing general experimental details, MOF syntheses, hydrogen analyses, and supporting analytical data is available. See DOI: **https://doi.org/10.1039/d5su00631g**.

Acknowledgements

The authors respectfully acknowledge support for this work from the University of New Brunswick. The authors would also

like to thank Dr Erin Adlakha at Saint Mary's University and Dr Chris McFarlane at the University of New Brunswick for micro-X-ray fluorescence measurements, Dr Kyle Rodgers at the University of New Brunswick for Thermogravimetric analysis. BAB is grateful for the support provided from the Natural Science and Engineering Council of Canada (RGPIN-2024-04793), New Brunswick Foundation for Innovation (NBIF) Climate Impact Fund (CIF-2023-006), and NBIF Strategic Opportunities Fund (SOF-2024-007).

References

1 X. You, Z. Xing, S. Jiang, Y. Zhu, Y. Lin, H. Qiu, R. Nie, J. Yang, D. Hui, W. Chen and Y. Chen, *Dev. Built. Environ.*, 2024, **17**, 100319.
2 D. Brough and H. Jouhara, *IJ Thermofluids*, 2020, **1–2**, 100007.
3 J. T. Kloprogge, L. V. Duong, B. J. Wood and R. L. Frost, *J. Colloid Interface Sci.*, 2006, **296**, 572–576.
4 A. R. Hind, S. K. Bhargava and S. C. Grocott, *Colloids Surf., A*, 1999, **146**, 359–374.
5 X. Li, Y. Liu and T. Zhang, *Waste Manage. Res.*, 2023, **41**, 1498–1511.
6 M. Mahinroosta and A. Allahverdi, *J. Environ. Manag.*, 2018, **223**, 452–468.
7 A. Meshram and K. K. Singh, *Resour. Conserv. Recycl.*, 2018, **130**, 95–108.
8 A. Kudyba, S. Akhtar, I. Johansen and J. Safarian, *JOM*, 2021, **73**, 2625–2634.
9 N. R. Canada, *Aluminum facts*, **https://natural-resources.canada.ca/our-natural-resources/minerals-mining/mining-data-statistics-and-analysis/minerals-metals-facts/aluminum-facts/20510**, accessed 4 April 2024.
10 S. O. Adeosun, AM, 2014, **3**, 6.
11 E. David and J. Kopac, *J. Hazard. Mater.*, 2012, **209–210**, 501–509.
12 M. Wang, S. Zhang, S. Du, J. Wang and B. Liu, *Resour., Conserv. Recycl.*, 2025, **220**, 108352.
13 W. J. Bruckard and J. T. Woodcock, *Int. J. Miner. Process.*, 2009, **93**, 1–5.
14 B. Lou, H. Shen, B. Liu, J. Liu and S. Zhang, *Constr. Build. Mater.*, 2023, **409**, 133989.
15 H. HogenEsch, D. T. O'Hagan and C. B. Fox, *npj Vaccines*, 2018, **3**, 51.
16 H.-K. Peng, X. Wang, T.-T. Li, C.-W. Lou, Y. Wang and J.-H. Lin, *Polym. Adv.*, 2019, **30**, 2045–2055.
17 I. Chen, S. K. Hwang and S. Chen, *Ind. Eng. Chem. Res.*, 1989, **28**, 738–742.
18 V. F. Yusuf, N. I. Malek and S. K. Kailasa, *ACS Omega*, 2022, **7**, 44507–44531.
19 B. M. Weckhuysen and J. Yu, *Chem. Soc. Rev.*, 2015, **44**, 7022–7024.
20 A. Meshram, A. Jain, M. D. Rao and K. K. Singh, *J. Mater. Cycles Waste Manage.*, 2019, **21**, 984–993.
21 M. Kale, I. H. Yılmaz, A. Kaya, A. E. Çetin and M. S. Söylemez, *J. Energy Inst.*, 2022, **100**, 99–108.
22 J. A. Scher, S. E. Weitzner, Y. Hao, T. W. Heo, S. T. Castonguay, S. Aubry, S. A. Carroll and M. P. Kroonblawd, *ACS Appl. Mater. Interfaces*, 2023, **15**, 28716–28730.
23 S. P. du Preez and D. G. Bessarabov, *Int. J. Hydrogen Energy*, 2021, **46**, 35790–35813.
24 S. S. Razavi-Tousi and J. A. Szpunar, *Int. J. Hydrogen Energy*, 2013, **38**, 795–806.
25 W. Tang, L. Yan, K. Li, Y. Juan, C. Fu and J. Zhang, *Mater. Today Commun.*, 2022, **31**, 103517.
26 A. Meshram, R. Jha and S. Varghese, *Mater. Today Proc.*, 2021, **46**, 1487–1491.
27 D. Belitskus, *J. Electrochem. Soc.*, 1970, **117**, 1097.
28 D. W. Hurtubise, D. A. Klosterman and A. B. Morgan, *Int. J. Hydrogen Energy*, 2018, **43**, 6777–6788.
29 E. J. Andersen, *US Pat.*, 7144567B2, 2003–2023.
30 C. F. Holder and R. E. Schaak, *ACS Nano*, 2019, **13**, 7359–7365.
31 H. A. Evans, D. Mullangi, Z. Deng, Y. Wang, S. B. Peh, F. Wei, J. Wang, C. M. Brown, D. Zhao, P. Canepa and A. K. Cheetham, *Sci. Adv.*, 2022, **8**, eade1473.
32 P. K. Kiyohara, H. S. Santos, A. C. V. Coelho and P. D. S. Santos, *An. Acad. Bras. Ciênc.*, 2000, **72**, 471–495.
33 F. Fathieh, M. J. Kalmutzki, E. A. Kapustin, P. J. Waller, J. Yang and O. M. Yaghi, *Sci. Adv.*, 2018, **4**, eaat3198.
34 N. Hanikel, M. S. Prévot, F. Fathieh, E. A. Kapustin, H. Lyu, H. Wang, N. J. Diercks, T. G. Glover and O. M. Yaghi, *ACS Cent. Sci.*, 2019, **5**, 1699–1706.
35 N. Hanikel, X. Pei, S. Chheda, H. Lyu, W. Jeong, J. Sauer, L. Gagliardi and O. M. Yaghi, *Science*, 2021, **374**, 454–459.
36 Z. Zheng, H. L. Nguyen, N. Hanikel, K. K.-Y. Li, Z. Zhou, T. Ma and O. M. Yaghi, *Nat. Protoc.*, 2023, **18**, 136–156.
37 M. Gaab, N. Trukhan, S. Maurer, R. Gummaraju and U. Müller, *Microporous Mesoporous Mater.*, 2012, **157**, 131–136.
38 J. Zhu, J. Hu, H. Xiao, L. Yang, M. Yang, S. Wang, J. Zhang and H. Xing, *Sep. Purif. Technol.*, 2024, **331**, 125614.
39 J. A. Coelho, A. M. Ribeiro, A. F. P. Ferreira, S. M. P. Lucena, A. E. Rodrigues and D. C. S. de Azevedo, *Ind. Eng. Chem. Res.*, 2016, **55**, 2134–2143.
40 J. Tang, G. Liu, T. Qi, Q. Zhou, Z. Peng, X. Li, H. Yan and H. Hao, *Hydrometallurgy*, 2022, **209**, 105836.
41 **https://www.un.org/en/exhibits/page/sdgs-17-goals-transform-world**.